Resveratrol induces ferroptosis to repress malignant progression of lung cancer cells

YUWEI WU[1*], NAN MA[2*], NING WANG[1], XINYU LIU[3], XIAOXUE MA[1], YANLEI GE[2] and JING CHEN[1]

[1]College of Life Sciences, North China University of Science and Technology, Tangshan, Hebei 063210, P.R. China;
[2]North China University of Science and Technology Affiliated Hospital, Tangshan, Hebei 063000, P.R. China;
[3]College of Basic Medicine, North China University of Science and Technology, Tangshan, Hebei 063210, P.R. China

Received March 31, 2026; Accepted October 14, 2026

DOI: 10.3892/or.2026.9219

Abstract. Lung cancer (LC) is a highly lethal malignancy arising from tracheobronchial mucosal or glandular epithelium, responsible for ~18% of global cancer mortality, with poor long-term patient survival. Resveratrol (Res, 445154), a natural polyphenol enriched in grapes, peanuts and *Polygonum cuspidatum*, exhibits robust anti-inflammatory and antioxidant effects. Since chronic inflammation promotes tumorigenesis, Res may restrain tumor progression via disrupting inflammatory cascades. This study aimed to evaluate Res-mediated suppression of proliferation, migration and invasion in LC cells, and delineate its roles in inducing apoptosis and ferroptosis. MTT, trypan blue exclusion and colony formation assays were used to assess the anti-proliferative effects of Res. Wound healing, Transwell migration and Matrigel invasion assays together with western blotting were performed to examine LC cell migration, invasion and related molecular mechanisms. Differentially expressed genes were screened from the Gene Expression Omnibus (GEO) datasets, followed by Kyoto Encyclopedia of Genes and Genomes pathway enrichment analysis to predict the potential cell death pathways modulated by Res. DCFH-DA staining, JC-1 assay, glutathione quantification, western blotting and ferrostatin-1 rescue experiments were performed to confirm Res-triggered ferroptosis. Functional experiments showed that Res markedly suppressed LC cell proliferation, migration and invasion via the epithelial-mesenchymal transition pathway and induced apoptosis. Bioinformatics analysis identified enrichment of the arachidonic acid metabolism pathway in Res-treated cells. Owing to the close link between arachidonic acid metabolism and ferroptosis, we hypothesized that Res triggers ferroptosis in LC cells, which was verified by cellular assays. In summary, Res exerts broad anti-tumor effects in LC cells by restraining proliferation, migration and invasion and stimulating apoptosis and ferroptosis.

Correspondence to: Professor Jing Chen, College of Life Sciences, North China University of Science and Technology, 21 Bohai Road, Caofeidian Xincheng, Tangshan, Hebei 063210, P.R. China
E-mail: chenjing@ncst.edu.cn

Professor Yanlei Ge, North China University of Science and Technology Affiliated Hospital, 73 Jianshe South Road, Lubei, Tangshan, Hebei 063000, P.R. China
E-mail: geyanlei@ncst.edu.cn

*Contributed equally

Key words: lung cancer, resveratrol, apoptosis, ferroptosis

Introduction

According to previous studies, the leading cause of death worldwide remains cancer, with more than 100 types of cancer currently identified. In 2022, 1.9 million new cancer cases were reported in the United States alone, resulting in more than 600,000 deaths. Among them, lung cancer (LC) and bronchial cancer are the deadliest. LC is the second most common cancer in the world after breast cancer (1). The number of new cases worldwide has reached 2.2 million, accounting for ~11.4% of all new cancer cases (2). Among them, 1.79 million patients with LC have succumbed, which is the highest death toll among all cancers (3). Patients with LC show a wide range of symptoms and signs, but there are no obvious diagnostic features in the early stages. Therefore, more than 70% of patients with LC are already in the late stage of LC when first diagnosed. There are few treatment methods, and the effects and prognosis are poor. Therefore, there is still an urgent need to discover new methods for the prevention, early diagnosis and treatment of LC to reduce the prevalence of LC and improve the survival rate of patients with LC.

Resveratrol (Res) occurs naturally in numerous plants such as peanuts, soybeans, grapes and berries (4,5). As the extensive biological properties of Res were discovered, a large number of studies related to Res were proposed. Currently, Res is considered to have various biological effects such as antioxidant, anti-inflammatory, cardioprotective, neuroprotective and anti-diabetic effects (6,7). Various studies have shown that Res is involved in numerous stages of cancer development and is considered a very promising drug to inhibit cancer development (8).

Ferroptosis is a form of cell death driven by iron-dependent accumulation of lipid peroxides, which is different from traditional forms of cell death such as apoptosis and necrosis (9).

Iron plays a crucial role in cellular metabolism because it is not only involved in oxygen transport and energy metabolism, but also in DNA synthesis and repair (10). However, excessive iron accumulation can lead to an increase in intracellular reactive oxygen species (ROS), thereby triggering oxidative stress, damaging cellular DNA and other macromolecules, and promoting tumor occurrence and progression (11) In recent years, increasing evidence has shown that iron metabolism disorders are closely related to the occurrence of various cancers, including LC.

In the present study, it was aimed to explore the regulatory effect of Res on the proliferation, migration and invasion of LC cells, and to further clarify whether it can induce apoptosis and ferroptosis in LC cells.

Materials and methods

Cell culture and reagents. Res was obtained from Sangon Biotech Co., Ltd. Human LC cell lines H460 and A549 were preserved in our laboratory. H460 cells were cultured in RPMI-1640 medium (cat. no. 03.4001C; Eallbio) supplemented with 10% fetal bovine serum (FBS; cat. no. 164210; Procell Life Science & Technology Co., Ltd.) and 1% penicillin-streptomycin solution (cat. no. Eallbio). A549 cells were maintained in DMEM (cat. no. 03.1002C; Eallbio) containing 10% FBS and 1% penicillin-streptomycin solution (Eallbio). All cell lines were incubated at 37˚C in a humidified atmosphere with 5% CO_2 (Thermo Fisher Scientific, Inc.).

MTT. A total of 4,000-6,000 LC cells/well was inoculated into a 96-well plate and cultured for 24 h at 37˚C and 5% CO_2. Then serum-free medium containing Res was added into the 96-well plate according to the concentration gradient and treated for 24-48 h. After the treatment was completed, MTT was added and incubation was continued for 4 h. Then DMSO was added to each well to dissolve the formed crystals, and the absorbance was measured at 570 nm. Calculations were performed using GraphPad 10.0 software (Dotmatics).

Based on the preliminarily determined IC_{50} values of Res in LC cells, gradient concentrations with low, medium and high inhibitory effects were selected for subsequent functional experiments, ensuring the rationality and reliability of the experimental dose design. The working concentration gradients of Res were set at 50, 100 and 150 μM for H460 cells; and 100, 150 and 200 μM for A549 cells.

Trypan blue and colony formation experiments. Trypan blue staining was used to detect cell viability. LC cells were seeded in a 6-well plate at a density of $5x10^5$ cells/well, serum-free medium containing Res was added, and incubated in a constant temperature incubator at 37˚C and 5% CO_2 for 48 h. Cells were collected from each well and transferred to a centrifuge tube. After centrifuging 800 x g at 37˚C for 3 min, the supernatant was discarded, 0.5% trypan blue dye was added, and stained at room temperature (RT) for 3 min. The staining of the cells was then observed under an inverted microscope, and the cell survival rate was calculated by counting the number of viable cells.

The colony formation assay was performed to evaluate the regulatory effect of Res on cell proliferation. Briefly, the treated cells were evenly seeded into 6-well plates at a density of 4,000 cells per well. After cell adherence, the cells were divided into different groups according to the experimental design. For H460 cells, the experimental groups included the blank control group, DMSO solvent control group, 50 μM Res group, 100 μM Res group, and 150 μM Res group. For A549 cells, the cells were assigned to the blank control group, DMSO solvent control group, 100 μM Res group, 150 μM Res group, and 200 μM Res group. All experiments were performed in at least three independent replicates. Subsequent culture was continued until most cell clusters contained ~50 cells. The cell colonies were then fixed with 4% paraformaldehyde at RT and stained with 1% crystal violet solution for 15-20 min. Finally, the colony formation status of each group was observed by optical microscope and recorded for statistical analysis.

Wound healing assay, migration and invasion experiments. LC cells in the logarithmic growth phase were seeded in a 6-well plate. When the cells were in favorable condition and full, a 100-μl pipette tip was used to perform a single fluid movement in the well plate to make cell scratches and rinsed with PBS to ensure that the scratched cells. The cells were cleaned with PBS and images of them were captured under an inverted microscope at 0 h. Then serum-free medium containing Res was added according to the groups. Each group had three duplicate wells. After culturing for 48 h, images of the scratch healing after 48 h at the same position at 0 h were captured under an inverted microscope. Subsequent analysis was performed using ImageJ 1.46r software (National institutes of Health).

Transwell invasion experiment. An equal volume of 100 μl 4 mg/ml Matrigel (cat. no. 354230; Corning, Inc.) was uniformly spread over the 8-μm pore size filter membrane of 24-well Transwell upper inserts and incubated at 37˚C to allow full solidification. Complete medium supplemented with 20% FBS was added to the lower chamber as a chemotactic attractant. Drug-treated cells were resuspended to prepare a single-cell suspension, and $1x10^4$ cells were seeded evenly into the upper chamber, followed by routine incubation for the preset duration.

After incubation, the culture medium in both upper and lower chambers was discarded, and the Transwell inserts were gently washed twice with sterile PBS. The invasive cells that penetrated the membrane were fixed with 4% paraformaldehyde at RT for 10 min and subsequently stained with 0.1% crystal violet solution for another 10 min. After removal of excess stain via gentle rinsing, the non-invasive cells remaining on the upper membrane surface were thoroughly wiped off using sterile wet cotton swabs. Finally, the migratory cells on the lower membrane surface were observed and images were captured under an inverted optical inverted microscope for subsequent quantitative analysis.

Hoechst 33342 fluorescent staining. The 1 mg/ml Hoechst 33342 fluorescent dye (cat. no. C1022; Beyotime Institute of Biotechnology) was diluted with serum-free medium to prepare a working concentration of 10 μg/ml. After drug intervention, 1 μl of the prepared working solution was gently added to each well containing 1 ml of serum-free medium. The plates were

subsequently incubated at 37˚C for 30 min in a humidified cell incubator. Finally, cell nuclear morphological changes were observed and imaged using a fluorescence microscope with an excitation wavelength of 377 nm and an emission wavelength of 447 nm.

Flow cytometry apoptosis assay. LC cells were cultured until the logarithmic growth phase and then subjected to drug treatment for 48 h. After the treatment, the culture medium was discarded, and the cells were rinsed twice with pre-cooled PBS buffer. The cells were resuspended in 1X binding buffer, and the cell density was adjusted to $1x10^6$ cells/ml. Subsequently, Annexin V-FITC and PI staining solutions were sequentially added to the cell suspension in accordance with the manufacturer's protocols of the flow cytometric apoptosis detection kit (cat. no. 556547; Becton, Dickinson and Company). After gentle mixing, the cell suspension was incubated at RT for 15 min in the dark. Following staining, the cells were rinsed with PBS again. Cell apoptosis was subsequently detected by a flow cytometer (CytoFLEX; Beckman Coulter, Inc.), and the acquired data were further analyzed using FlowJo 10.9 software (FlowJo LLC).

Bio-information prediction. Two gene expression datasets GSE9008 (12) and GSE41445 (13) concerning Res-treated A549 LC cells were retrieved from the Gene Expression Omnibus (GEO) database (https://www.ncbi.nlm.nih.gov/gds). Batch effects between the two datasets were eliminated using the sva package in R software (https://bioconductor.org/packages/sva). The Limma package was subsequently applied to screen differentially expressed genes (DEGs) with the threshold values of $|logFC|>0.5$ and adjusted $P<0.05$. Finally, Kyoto Encyclopedia of Genes and Genomes (KEGG) pathway enrichment analysis was performed to explore the potential functional pathways of the identified DEGs.

ROS detection. The instructions of the Report Biotech ROS detection kit (cat. no. RK1002; Reportbio; http://www.ruipate.com/) was followed. The DCFH-DA reagent (10 mM) was first diluted 1,000-fold with serum-free culture medium to prepare a working solution; after aspirating the original culture solution in the 6-well plate, 1 ml of DCFH-DA working solution was added to each well for staining. After staining was completed, the working solution in the well was aspirated and the cells were washed three times with serum-free medium to ensure complete removal of free DCFH-DA reagent. They were then observed and images were captured under an inverted fluorescence microscope. A fluorescence channel with an excitation wavelength of 488 nm and an emission wavelength of 525 nm was selected to quantitatively detect the fluorescence intensity of cells after drug stimulation through flow cytometry to reflect ROS levels.

To further confirm that Res induces ferroptosis in LC cells, rescue experiments were conducted using the ferroptosis inhibitor Ferrostatin-1 (Fer-1; cat. no. 17729; Cayman Chemical Company). The experiment comprised four groups: A blank control group (C), a DMSO solvent control (DMSO), a Res monotherapy group (Res), and a Res combined with Fer-1 group (Fer-1 + Res). The LC cells were treated with Res at the 48-h IC_{50} concentration and incubated for 48 h. For the Fer-1 + Res group, the cells were treated with Res and 1 mM Fer-1 working solution for 48 h.

JC-1 staining assay for mitochondrial membrane potential (MMP). JC-1 staining solution (cat. no. HY-15534; MedChemExpress) was added to 6-well plates containing drug-treated cells at a final concentration of 10 mM. The plates were incubated at 37˚C for 15 min under dark conditions. To prevent dye aggregation during incubation, the culture plates were gently shaken every 4 min. Upon completion of incubation, the staining solution was aspirated, and the cells were gently rinsed twice with PBS to thoroughly remove unbound JC-1 dye. The cellular fluorescence alterations were subsequently observed and captured using a fluorescence microscope for subsequent qualitative and quantitative analysis.

Glutathione (GSH) level detection assay. Cells in the logarithmic growth phase were seeded into 6-well plates and subjected to corresponding drug treatment. Subsequently, the cells were collected, and the detection reagent was prepared and added strictly in accordance with the operating instructions of the GSH Level Detection Kit (cat. no. S0052; Beyotime Institute of Biotechnology). The absorbance of each sample was measured at a wavelength of 412 nm using a microplate reader. Finally, the relative GSH levels of all groups were calculated, followed by statistical analysis and graphical visualization.

Western blotting. Total cellular proteins were extracted using RIPA lysis buffer (cat. no. P0013D; Beyotime Institute of Biotechnology), and protein concentrations were determined via a BCA protein quantification kit (cat. no. ZJ102; Epizyme) following the manufacturer's protocols. 10 μg of protein per well was separated by 10% SDS-PAGE and subsequently electro-transferred onto a PVDF membrane (MilliporeSigma).The membranes were blocked with skim milk powder (Becton, Dickinson and Company) for 2 h at RT and then thoroughly rinsed with 1X TBST (containing 0.1% Tween-20) three times for 10 min each. Protein bands were visualized and band densitometric analysis was performed using ImageJ software.

Subsequently, the membranes were incubated with diluted primary antibodies overnight at 4˚C. The primary antibodies and corresponding dilution ratios were as follows: Anti-β-actin (1:20,000; cat. no. AC026; ABclonal Biotech Co., Ltd.), anti-GAPDH (1:5,000; cat. no. ET1601-4; Huabio), anti-E-cadherin (1:500; cat. no. 0407-25; Huabio), anti-Slug (1:1,000; cat. no. HA722828; Huabio), anti-Snail (1:1,000; cat. no. ER1706-22; Huabio), anti-P53 (1:2,000; cat. no. SA39-07 Huabio), anti-Bcl-2 (1:2,000; cat. no. SA10-03; Huabio), anti-BAX (1:1,000; cat. no. SZ3-07; Huabio), anti-SLC7A11 (1:1,000; cat. no. HA721868; Huabio), anti-GPX4 (1:10,000; cat. no. ET1706-45; Huabio), and anti-ACSL4 (1:500; cat. no. T510198; Abmart Pharmaceutical Technology Co., Ltd.). After extensive washing with 1X TBST, the membranes were incubated with horseradish peroxidase-conjugated secondary antibodies (goat anti-rabbit IgG; 1:5,000; cat. no. BR70004; ABclonal Biotech Co., Ltd.) at RT for 1 h. Finally, protein bands were visualized using ECL ultrasensitive luminescent solution (cat. no. P1050; Applygen

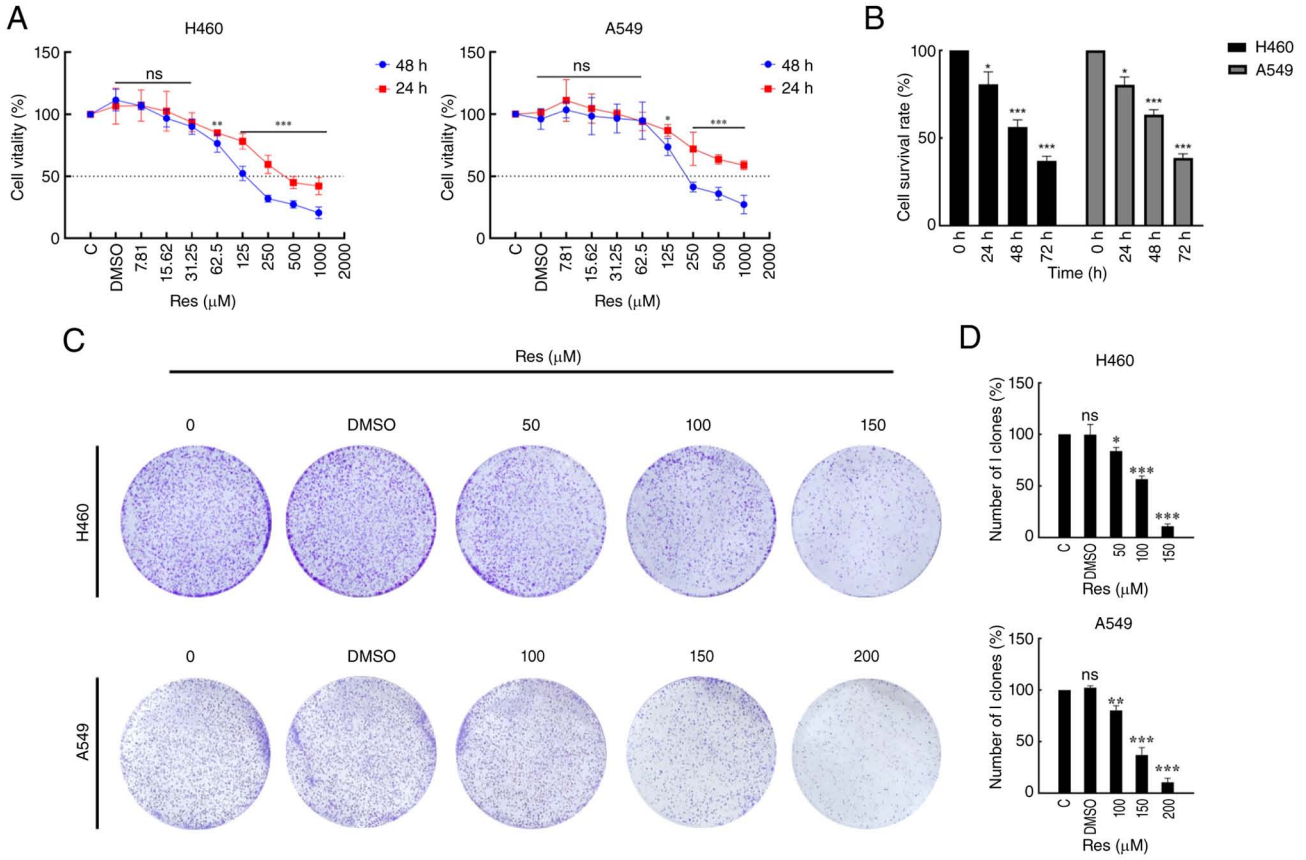


Figure 1. Effect of Res on LC cell proliferation. (A) MTT assay to assess the survival rate of LC cell lines treated with Res. (B) Trypan Blue experiment detects the effect of Res on cell viability. (C and D) Colony formation experiment to detect the effect of Res on cell proliferation ability and calculated in histogram. Data are presented as the mean ± SD. Data are representative of three independent experiments. *P<0.05, **P<0.01 and ***P<0.001. Res, resveratrol; LC, lung cancer; ns, no significance.

Technologies, Inc.) with a chemiluminescence imaging system (SH-Compact 523; Shenhua Science Technology Co., Ltd.).

Statistical methods. In the present study, R language (version 4.4.0) was utilized to analyze data in bioinformatics. All experiments were performed in at least three independent biological replicates. Data are presented as the mean ± standard deviation (SD). Differences between two groups were compared using unpaired Student's t-test and comparisons among three or more groups were performed with one-way or two-way ANOVA followed by Tukey's post hoc test for multiple comparisons. All plots and graphs were generated using GraphPad Prism version 10.2.3 (Dotmatics).

Results

Effect of Res on LV cell proliferation. In order to explore the effect of Res on the proliferation of LC H460 and A549 cells, different concentrations (0, 7.81, 15.62, 31.25, 62.5, 125, 250, 500, 1,000 and 2,000) Res and DMSO control group treated LC H460 and A549 cells for 24 and 48 h. The MTT method was used to determine the effect of Res on the proliferation of human LC cells. Experimental results showed that compared with the 0 μM group, Res could significantly inhibit the proliferation of LC cells H460 and A549, induce LC cell death, and show a time-dependent and concentration-dependent trend (Fig. 1A). Statistical analysis revealed that the optimal drug concentrations of Res for H460 were 155.17±2.14 and 81.31±1.64 μM at 24 and 48 h respectively, and the optimal drug concentrations for A549 were 193.33±2.36 and 147.27±1.96 μM at 24 and 48 h respectively. The IC_{50} value at 48 h was determined, and concentrations around this IC_{50} (including lower and higher doses) were selected for subsequent functional experiments.

Trypan blue can penetrate damaged cell membranes and stain dead cells blue. Therefore, the trypan blue assay was used to detect the survival rates of H460 and A549 cells after Res treatment for 0, 24, 48 and 72 h. The results demonstrated that when the drug concentration was the same, the cell survival rate gradually decreased with the increase of treatment time. Combined with the results of the MTT experiment, 48 h was selected as the drug action time for subsequent experiments (Fig. 1B).

Clone formation assay is used to detect the long-term proliferation ability of cells. H460 cells and A549 cells were treated with 0, DMSO control, 50, 100 and 150 μM and 0, DMSO, 100, 150 and 200 μM Res for 48 h, respectively. The results showed that after treatment with Res, the number of colonies formed by the two cells was significantly reduced (Fig. 1C and D), proving that Res can inhibit the proliferation of LC cells.

Effect of Res on migration and invasion of LC cells. To verify whether Res is related to the migration and invasion of LC

cells. The changes in cell migration ability of the two cell lines after treatment with Res were detected by scratch assay. The results showed that compared with the control group, the scratch healing area gradually decreased with increasing drug concentration (Fig. 2A and B), indicating that Res inhibited the migration ability of H460 and A549 cells in a dose-dependent manner.

Based on the results of the scratch experiment, the Transwell migration experiment was used for verification. The experimental results revealed that the number of cell migration decreased with increasing drug concentration, which was consistent with the results of the scratch experiment (Fig. 2C and D), further proving that Res inhibits the migration ability of LC cells. The aforementioned results identify that Res can inhibit the migration ability of LC H460 and A549 cells, and as the drug concentration increases, the inhibitory effect becomes more obvious.

In order to verify the effect of Res on the invasion ability of LC cells, a Transwell invasion experiment was performed. The results showed that the number of cell migration was reduced after drug treatment (Fig. 2E and F). Res inhibited the invasive ability of LC cells.

Effect of Res on the expression of epithelial-mesenchymal transition (EMT)-related proteins in LC cells. EMT is closely related to migration and invasion. Related proteins were detected by western blot experiment. The results demonstrated that compared with the control group, the expression of EMT-related protein E-cadherin in the drug-treated group was significantly increased, and the expression levels of slug and snail were significantly reduced (Fig. 2G and H). Combining the results of scratch assay and Transwell migration and invasion assay, Res can inhibit the migratory and invasive ability of H460 and A549 cells through the EMT pathway.

Effect of Res on apoptosis of LC cells. In order to explore whether Res induces apoptosis in LC cells, H460 and A549 were treated with different concentrations of Res and then stained with Hoechest 33342. The results revealed that the cells treated with Res showed strong blue fluorescence and obvious apoptotic bodies (Fig. 3A). Cell apoptosis was detected by flow cytometry, and it was found that the proportion of apoptotic cells gradually increased as the drug concentration increased (Fig. 3B and C). Western blot was used to detect the expression of apoptosis-related proteins to further verify that Res induces apoptosis in LC cells. The results identified that Res upregulated the protein expression of BAX and p53 and reduced the expression of Bcl-2 protein (Fig. 3D and E). Based on the aforementioned experiments, it is confirmed that Res promotes apoptosis of LC cells.

Bioinformatics predicts the mechanism of Res-induced LC cell death. After de-batch correction of the two data sets GSE9008 and GSE41445 in the GEO database, DEGs were screened, and a total of 1,455 differential genes were obtained. KEGG pathway enrichment analysis was performed on the differential genes, and the results showed that the arachidonic acid metabolism pathway was significantly enriched (Fig. 4A and B). Combined with the close relationship between the arachidonic acid pathway and ferroptosis, it is hypothesized that Res may induce ferroptosis in LC cells by regulating this pathway.

Effect of Res on ferroptosis in LC cells. Ferroptosis is a programmed cell death driven by iron-dependent lipid peroxidation that plays a crucial role in tumor development. In order to explore the effect of Res on ferroptosis in LC cells, the DCFH-DH probe was used to detect the accumulated level of ROS in LC cells after treatment with Res. The results showed that ROS levels in LC cells increased significantly after treatment with Res (Fig. 5A).

The occurrence process of ferroptosis is accompanied by specific changes in MMP, thus the JC-1 fluorescent probe is also one of the important indicators for detecting ferroptosis. The results revealed that the reduction in MMP caused the JC-1 probe to change from red fluorescence to green (Fig. 5B), proving that the MMP was reduced in LC cells after Res treatment, and Res induced ferroptosis in LC cells.

Further exploring the changes in GSH content in LC cells, it was found that the intracellular GSH content was significantly reduced after Res treatment (Fig. 5C). Based on flow cytometry, it was further demonstrated that ROS levels in LC cells increased after Res treatment (Fig. 5D). Western blot assays were carried out to confirm Res-mediated ferroptosis in LC cells by measuring the abundance of ferroptosis marker proteins. Elevated Res concentrations progressively downregulated SLC7A11 and GPX4, whereas ACSL4, a critical mediator of arachidonic acid metabolism, exhibited dose-dependent upregulation (Fig. 5E and F). The aforementioned experiments collectively proved that Res induced ferroptosis in LC cells.

In order to clarify whether Res can induce ferroptosis in LC cells, a ferroptosis inhibitor (Fer-1) intervention group was added to the system of Res-treated LC cells to conduct a rescue experiment. The results demonstrated that when Fer-1 was added after Res treatment, compared with the drug-treated group alone, the green fluorescence of the DCFH-DA fluorescent probe decreased (Fig. 6A), and the ROS content decreased; the green fluorescence of the JC-1 probe decreased, and the MMP in LC cells increased (Fig. 6B); GSH content detection found that after adding Fer-1, the GSH content increased (Fig. 6C); flow cytometric detection of ROS levels also showed that after Fer-1 treatment, ROS levels decreased compared with the Res treatment group alone (Fig. 6D). To further validate this regulatory effect, western blotting was performed to detect the ferroptosis-associated proteins SLC7A11, GPX4 and ACSL4. Compared with cells treated with Res alone, co-administration of Fer-1 restored the protein abundances of SLC7A11 and GPX4, while significantly downregulating ACSL4 expression in Res-exposed LC cells (Fig. 6E and F). In summary, Fer-1 may inhibit Res-induced ferroptosis by regulating cellular redox balance.

Discussion

Res primarily exerts its cytotoxic effects by activating the canonical TP53-dependent apoptosis pathway. It inhibits the migratory and invasive abilities of LC cells through the EMT pathway, while simultaneously inducing ferroptosis within these cells. Consequently, Res demonstrates significant antitumor activity (Fig. 7).

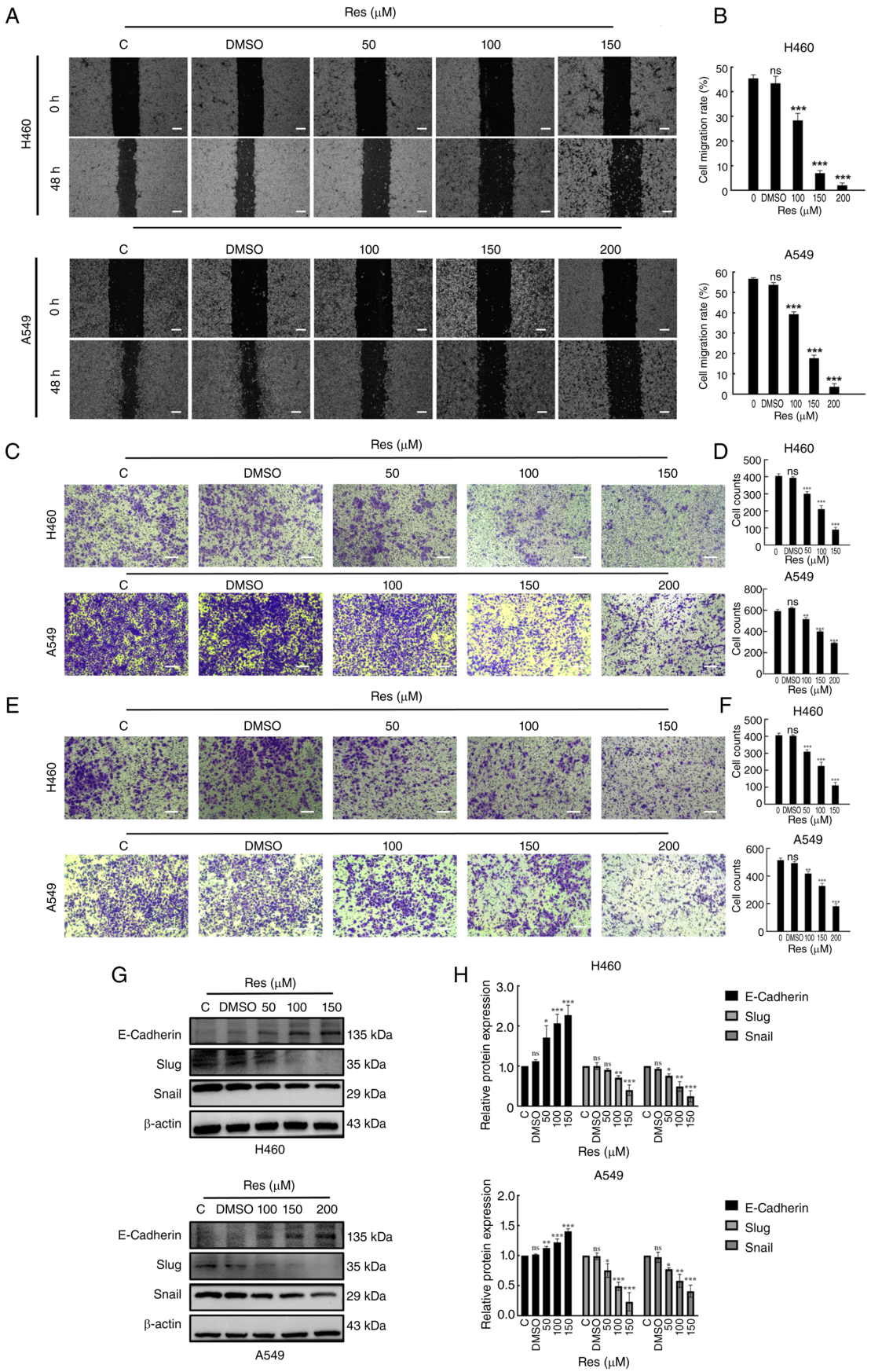


Figure 2. Effect of Res on migration and invasion of LC cells. (A and B) Wound healing assay for detecting the effect of Res on LC cell migration and calculated in histogram. (C and D) Transwell migration assays were used to assess cell migration ability (magnification, x100) and calculated in histogram. Scale bar, 100 μm. (E and F) Transwell invasion assays were used to evaluate cell invasion ability (magnification, x100) and calculated in histogram. Scale bar, 100 μm. (G and H) Western blot analysis was used to detect the expression of epithelial-mesenchymal transition-related proteins and calculated in histogram. Data are representative of three independent experiments. Data are representative of three independent experiments. *P<0.05, **P<0.01 and ***P<0.001. Res, resveratrol; LC, lung cancer; ns, no significance.

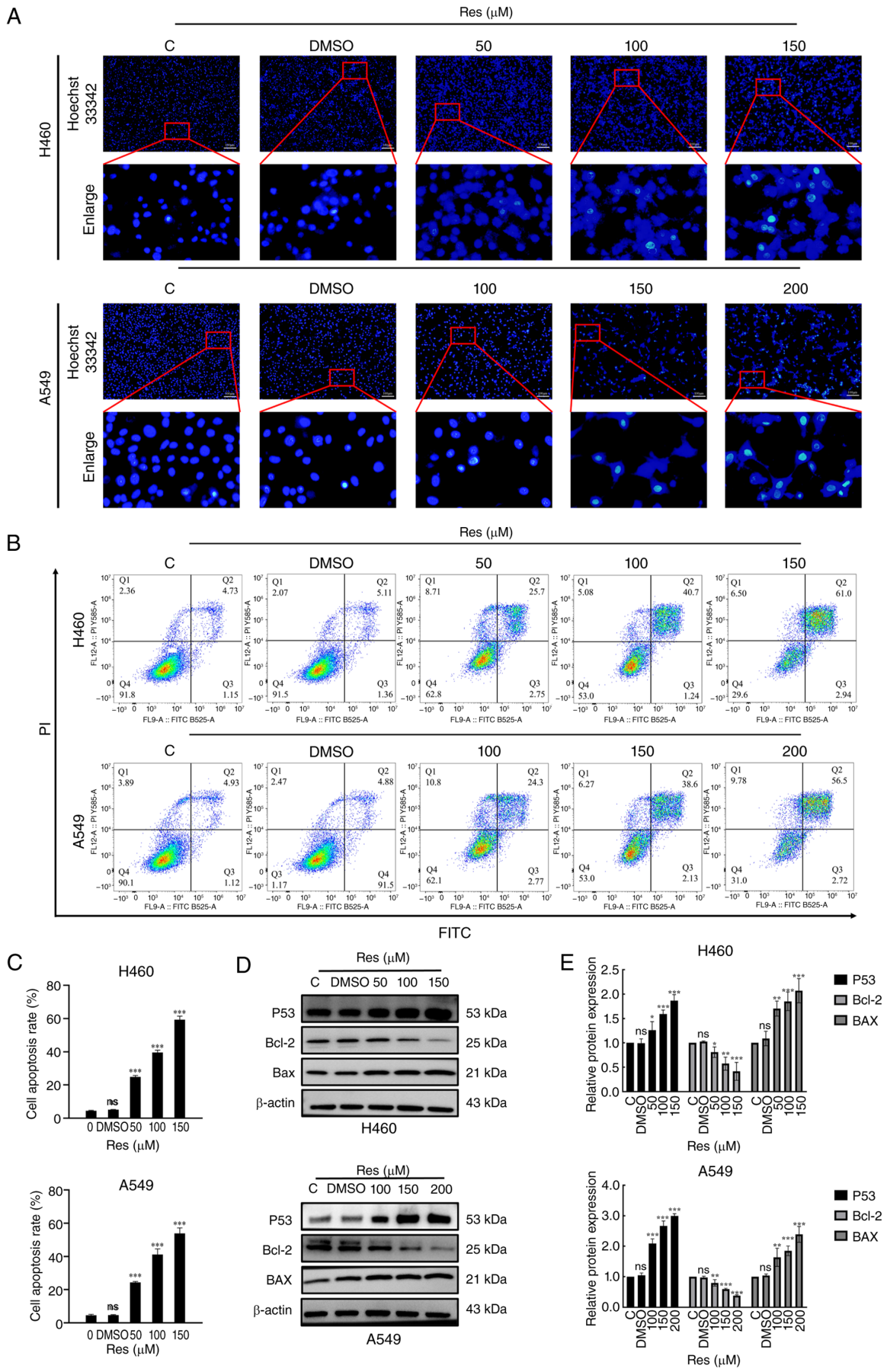


Figure 3. Effect of Res on apoptosis of lung cancer cells. (A) Hoechest 33342 fluorescence detection of changes in cellular apoptosis (magnification, x100). Scale bar, 100 μm. (B and C) Flow cytometric detection of changes in the proportion of apoptotic cells and calculated in histogram. (D and E) Western blot analysis of the expression of apoptosis-related proteins and calculated in histogram. Data are representative of three independent experiments. *P<0.05, **P<0.01 and ***P<0.001. Res, resveratrol; ns, no significance.

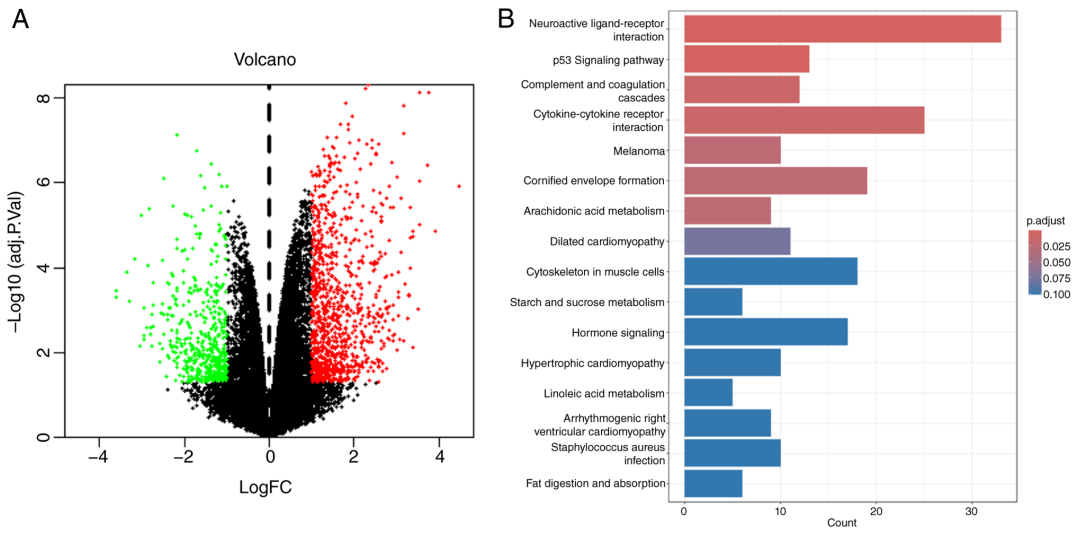


Figure 4. Bioinformatics predicts the mechanism of resveratrol-induced lung cancer cell death. (A) Volcano plot of DEGs. (B) Kyoto Encyclopedia of Genes and Genomes pathway enrichment analysis of DEGs. DEGs, differentially expressed genes.

Despite advances in understanding of LC risk, development, immune control and treatment options, it remains a leading cause of cancer death (14,15) and poses a significant threat to global public health (16). Most patients are already at an advanced stage when diagnosed, and chemotherapy and radiotherapy are the conventional main treatments for patients with cancer. However, after a period of treatment, most cancer cells will develop resistance to chemotherapy and radiotherapy, in addition to fatal side effects, with extremely low survival rates. Therefore, there is an urgent need to find new drugs and methods (17).

Res is a natural phenolic with a variety of biological effects, including antioxidant, anti-inflammatory, anticancer, cardioprotective, neuroprotective and anti-diabetic activities (18-20). It is also a phytoalexin produced by a variety of plants when they are injured or attacked by pathogens such as bacteria and fungi. It plays a key role in plant defense against stressful environments. Under stress, plants often trigger Res biosynthesis, thereby increasing its content (21,22). Res is a potent inducer of multiple tumor control (23) and is expected to improve cancer and drive breakthroughs in cancer treatment (24). Numerous studies indicate that Res offers a wide range of preventive and therapeutic options for different types of cancer. Furthermore, Res is widely considered to be useful in anticancer treatment in combination with other chemotherapeutic drugs and has received widespread attention for its potential as a chemo-preventive agent against human cancer (25). Therefore, the effect of Res on cancer cells has also become the subject of some studies (26).

Ferroptosis is a non-apoptotic cell death mechanism characterized by iron-dependent lipid peroxidation (27). The iconic feature under the electron microscope is the specific morphological changes of mitochondria, including increased membrane density and reduced mitochondrial cristae (28,29). It is morphologically, biochemically and genetically different from apoptosis, necrosis and autophagy (30), and as an innate tumor suppressive mechanism, it participates in the biological process of tumors (31). The rapid development of research on ferroptosis in cancer has enhanced its application prospects in cancer treatment (32). Intracellular iron accumulation and lipid peroxidation are the two major biochemical events leading to ferroptosis. Organelles, including mitochondria and lysosomes, are involved in the regulation of redox imbalance in iron metabolism and ferroptosis (33). ROS mediate lipid peroxidation to produce 4-hydroxyalkenal and other related products, which play a key role in the initiation of ferroptosis (34,35). GSH is an important member of the cellular antioxidant system. In cancer cells, high levels of GSH are crucial for clearing excess ROS. The loss of GSH will disrupt the redox homeostasis, leading to the accumulation of ROS, and ultimately triggering cell dysfunction and death. The higher oxidative stress in cancer cells renders them more sensitive to GSH deficiency. This feature can be used for cancer treatment (36-38).

The results confirmed that Res treatment inhibited the proliferative capacity of LC cells, attenuated the migratory and invasive abilities of these cells via the EMT pathway, and simultaneously induced apoptosis and ferroptosis in the cells.

In terms of clinical application prospects, the results of the present study provide key experimental support for the clinical transformation of Res: On the one hand, as a natural product, Res has the advantages of low toxicity and favorable biocompatibility. Compared with traditional chemotherapy drugs, it is more suitable for long-term intervention and is expected to be developed as an adjuvant treatment drug for patients with advanced LC. It can enhance chemotherapy sensitivity and reduce chemotherapy side effects by inducing ferroptosis; on the other hand, based on the present study, it is clear that based on its mechanism of action, combined treatment options targeting the ferroptosis pathway can be further developed, such as the combined use of Res with iron chelators, GSH synthesis inhibitors and other drugs to achieve precise targeted elimination of LC cells. In addition, the preventive potential of Res in chemotherapy can be extended to early intervention for high-risk groups of LC (such as long-term smokers and occupational exposure groups), reducing the incidence of LC by inhibiting cell proliferation and blocking the carcinogenesis process.

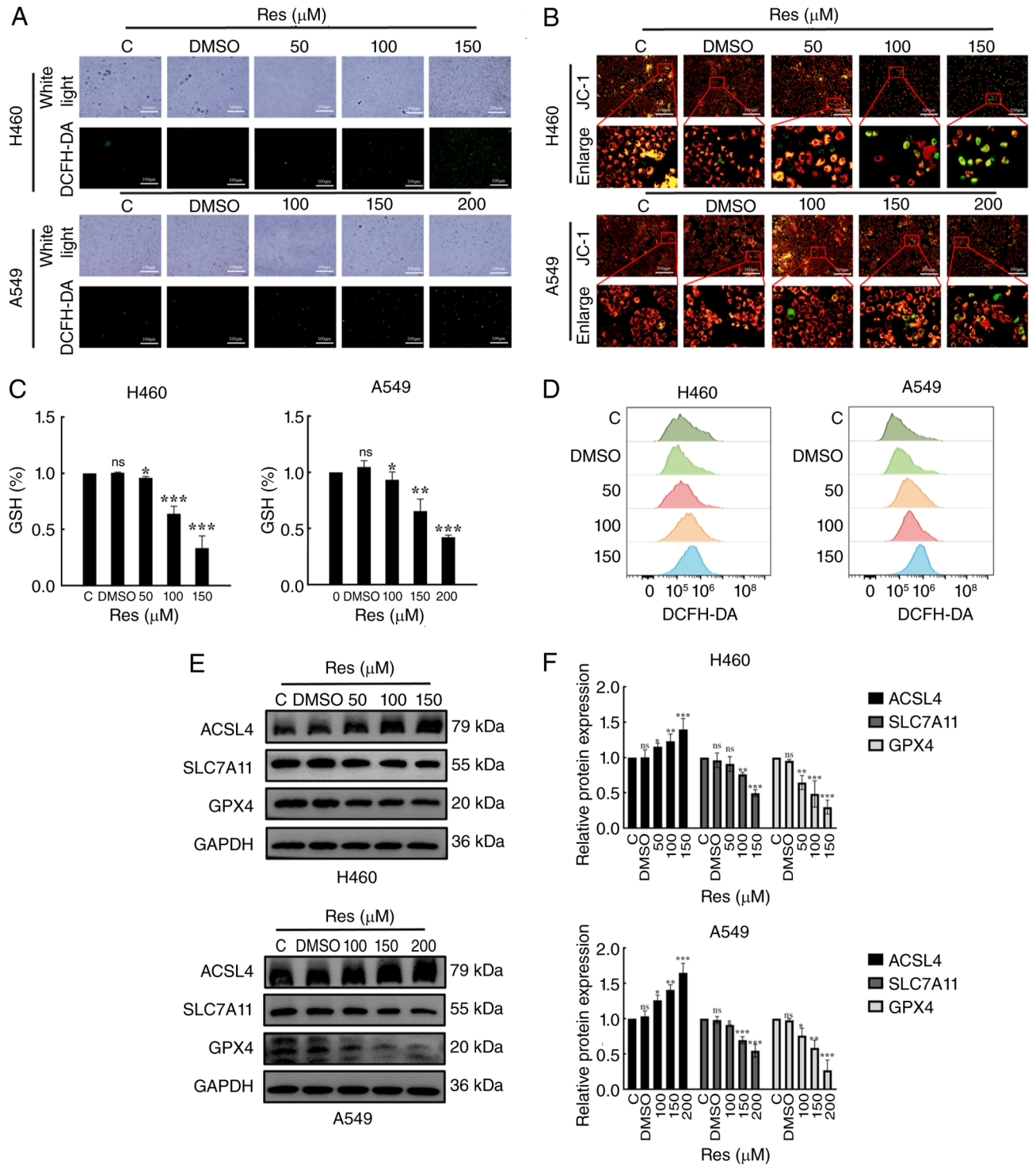


Figure 5. Effect of Res on ferroptosis in lung cancer cells. (A) DCFH-DA fluorescence detection of ROS changes in cells (magnification, x100). Scale bar, 100 μm. (B) JC-1 fluorescence detection of changes in the mitochondrial membrane potential of cells (magnification, x100). Scale bar, 100 μm. (C) Changes in the GSH content. (D) Flow cytometry detection of ROS changes in cells. (E and F) Western blot analysis of the expression of ferroptosis-related proteins and calculated in histogram. Data are representative of three independent experiments. *P<0.05, **P<0.01 and ***P<0.001. Res, resveratrol; ROS, reactive oxygen species; GSH, glutathione; ns, no significance.

Collectively, numerous published studies have documented the antitumor properties of Res in non-small cell LC (NSCLC), with most mechanistic investigations centering on its capacity to trigger intrinsic or extrinsic apoptotic pathways. Emerging research has preliminarily noted Res-induced ferroptosis in lung tumor cells, yet key limitations persist across existing literature. Most previous studies examine apoptosis or ferroptosis in isolation without dissecting their simultaneous activation and mutual crosstalk, few integrate public transcriptomic datasets to identify upstream lipid metabolic signaling governing Res-elicited ferroptosis, and studies linking Res to arachidonic acid metabolism in LC remain sparse.

Multiple previous studies have confirmed the antitumor capacity of Res in NSCLC, and several findings of the present

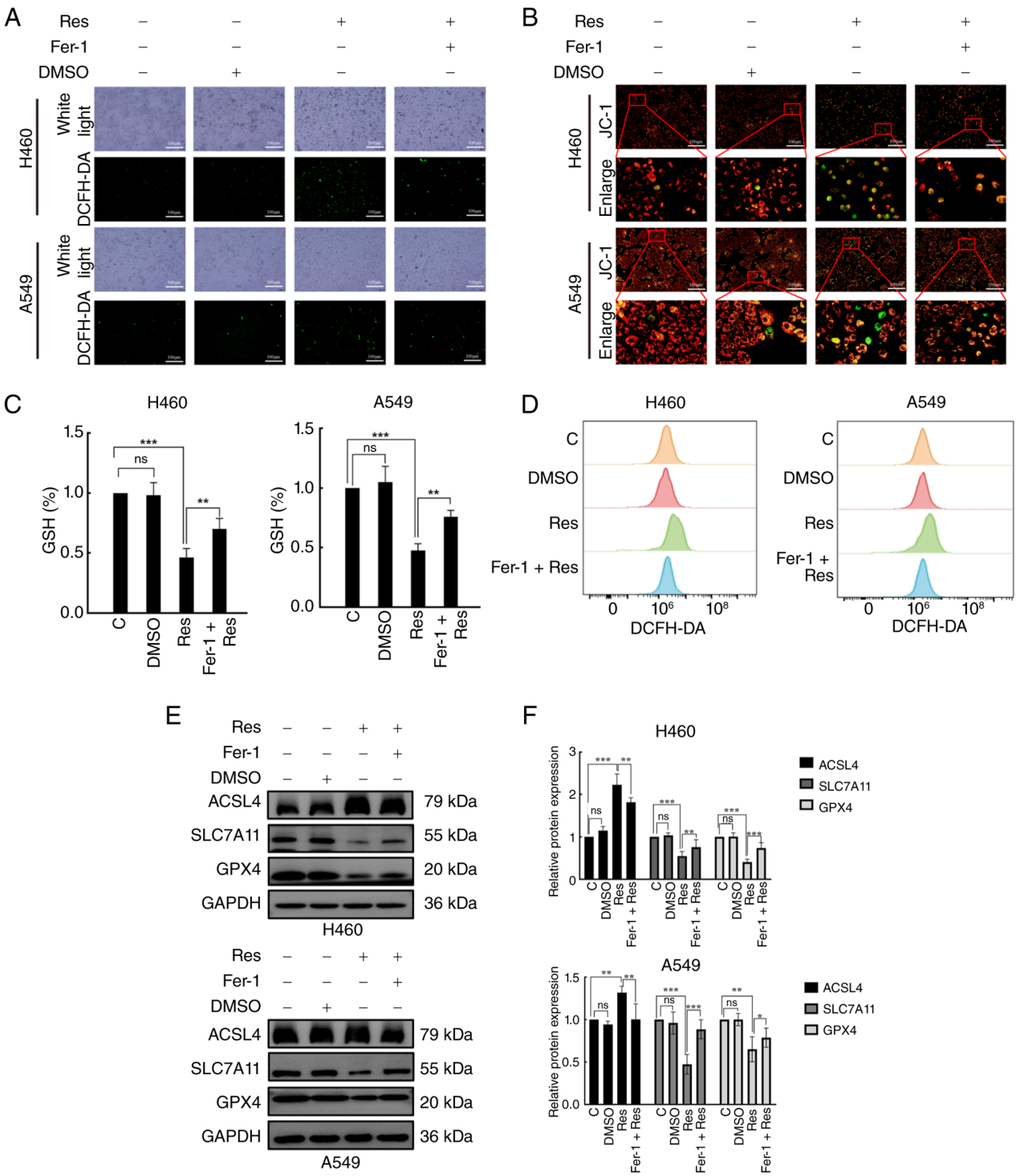


Figure 6. Effect of Res and ferrostatin-1 on ferroptosis in lung cancer cells. (A) DCFH-DA fluorescence detection of ROS changes in cells (magnification, x100). Scale bar, 100 μm. (B) JC-1 fluorescence detection of changes in the mitochondrial membrane potential of cells (magnification, x100). Scale bar, 100 μm. (C) Changes in the GSH content. (D) Flow cytometric detection of ROS changes in cells. (E and F) Western blot analysis of the expression of ferroptosis-related proteins and calculated in histogram. Data are representative of three independent experiments. *P<0.05, **P<0.01 and ***P<0.001. Res, resveratrol; ROS, reactive oxygen species; GSH, glutathione; ns, no significance.

study are consistent with these published results. In agreement with previous studies, Res was validated to induce apoptotic cell death, inhibit EMT progression, and elevate intracellular oxidative stress in NSCLC cells, which are well-recognized anticancer phenotypes of Res in LC research. With regard to ferroptosis regulation, existing NSCLC studies primarily focused on the inhibitory effect of Res on the SLC7A11/GPX4 antioxidant system, which sensitizes NSCLC cells to ferroptotic cell death. Consistent with these studies, the present results also verified that Res significantly downregulates SLC7A11 and GPX4 expression in NSCLC cells.

Nevertheless, the present study provides several extended and novel findings compared with current literature. First, most previous studies only partially focused on either

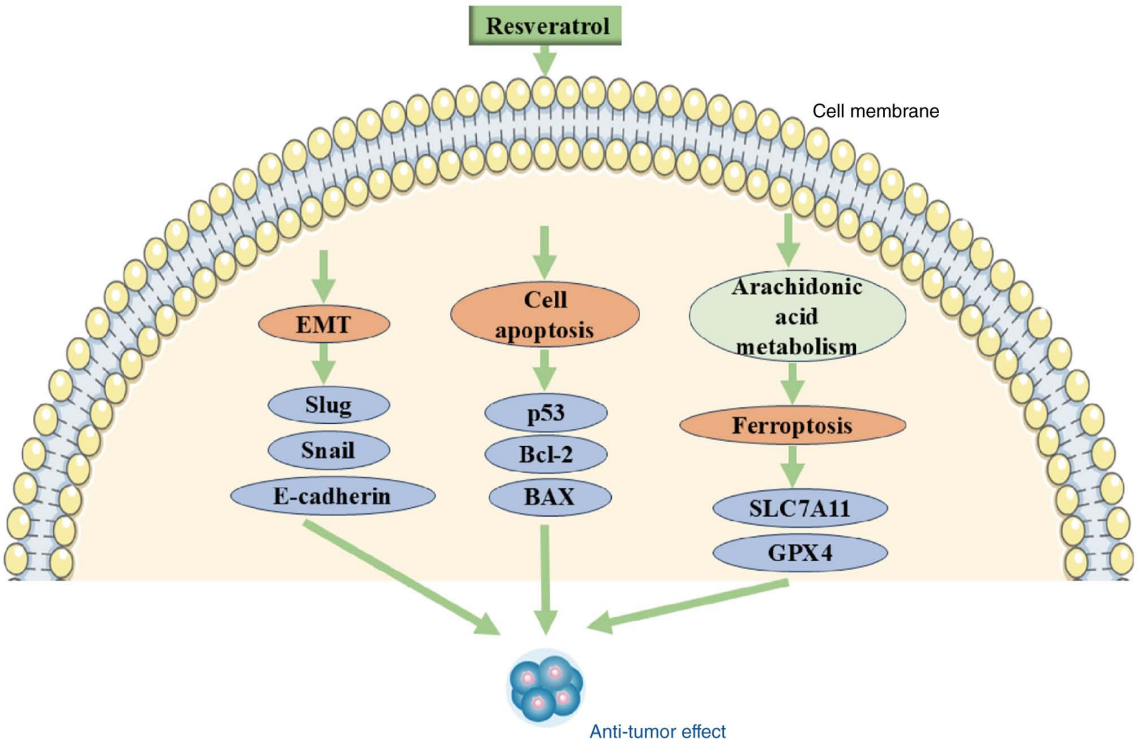


Figure 7. Mechanism diagram of resveratrol-mediated antitumor effects. EMT, epithelial-mesenchymal transition.

Res-induced apoptosis or ferroptosis in NSCLC, while few studies clarified the simultaneous activation of these two cell death patterns. Second, prior Res-ferroptosis studies in NSCLC rarely involved the regulation of ACSL4, a core pro-ferroptosis lipid-metabolizing enzyme. The current data further extends existing knowledge by demonstrating that Res markedly increases ACSL4 expression in NSCLC, thereby promoting lipid peroxidation and facilitating ferroptosis. Most importantly, an integrated regulatory network in NSCLC was established: Res suppresses the SLC7A11/GPX4 antioxidant defense while activating ACSL4-mediated lipid peroxidation, thereby enhancing oxidative stress, inhibiting EMT, and triggering concurrent apoptosis and ferroptosis. Unlike previous single-mechanism studies, this multi-pathway synergistic regulatory mode in NSCLC represents the specific and novel contribution of the present study.

Acknowledgements

Not applicable.

Funding

The present study was supported by the 2024 Government-Funded Program for Training Outstanding Talent in Clinical Medicine (grant no. ZF2024193) and the Key Scientific Research Project of North China University of Science and Technology (grant no. ZD-YG-202312).

Availability of data and materials

The data generated in the present study are included in the figures and/or tables of this article.

Authors' contributions

YW and NM conducted the experiments and wrote the manuscript. JC and YG conceived and designed the study, provided research guidance, and critically revised the manuscript for important intellectual content. NW, XL and XM participated in data analysis and summarized processed figures. YW and NM confirm the authenticity of all raw data. All authors read, critically revised and approved the final version of the manuscript, and agreed to be accountable for all aspects of this work.

Ethics approval and consent to participate

Not applicable.

Patient consent for publication

Not applicable.

Competing interests

The authors declare that they have no competing interests.

References

1. Kabir SR, Alam MT and Uddin MB: Asparagus racemosus silver chloride nanoparticles and Kaempferia rotunda mediated silver/silver chloride nanoparticles inhibit human hepatocellular and lung cancer cell lines. Biochem Biophys Rep 40: 101818, 2024.
2. Li Y, Sun Y, Jia B, Ma Z and Zhou R: MED23 depletion induces premature senescence in NSCLC cells by interacting with BCLAF1 and then suppressing NUPR1 expression. Biochem Biophys Res Commun 734: 150754, 2024.

3. Liu Y, Qing B, Ke W and Wang M: MEK inhibitor trametinib combined with PI3K/mTOR inhibitor BEZ-235 as an effective strategy against NSCLC through impairment of glucose metabolism. Cell Signal 124: 111415, 2024.
4. Breuss JM, Atanasov AG and Uhrin P: Resveratrol and its effects on the vascular system. Int J Mol Sci 20: 1523, 2019.
5. Galiniak S, Aebisher D and Bartusik-Aebisher D: Health benefits of resveratrol administration. Acta Biochim Pol 66: 13-21, 2019.
6. Qian W, Xiao Q, Wang L, Qin T, Xiao Y, Li J, Yue Y, Zhou C, Duan W, Ma Q and Ma J: Resveratrol slows the tumourigenesis of pancreatic cancer by inhibiting NFκB activation. Biomed Pharmacother 127: 110116, 2020.
7. Almatroodi SA, Alsahli MA, Aljohani ASM, Alhumaydhi FA, Babiker AY, Khan AA and Rahmani AH: Potential therapeutic targets of resveratrol, a plant polyphenol, and its role in the therapy of various types of cancer. Molecules 27: 2665, 2022.
8. Pawłowski W, Caban M and Lewandowska U: Cancer prevention and treatment with polyphenols: Type IV collagenase-mediated mechanisms. Cancers(Basel) 16: 3193, 2024.
9. Wang W, Xie Y and Malhotra A: Potential of curcumin and quercetin in modulation of premature mitochondrial senescence and related changes during lung carcinogenesis. J Environ Pathol Toxicol Oncol 40: 53-60, 2021.
10. Luo L, Wang H, Tian W, Zeng J, Huang Y and Luo H: Targeting ferroptosis for cancer therapy: Iron metabolism and anticancer immunity. Am J Cancer Res 11: 5508-5525, 2021.
11. Zhang YY, Han Y, Li WN, Xu RH and Ju HQ: Tumor iron homeostasis and immune regulation. Trends Pharmacol Sci 45: 145-156, 2024.
12. Whyte L, Huang YY, Torres K and Mehta RG: Molecular mechanisms of resveratrol action in lung cancer cells using dual protein and microarray analyses. Cancer Res 67: 12007-12017, 2007.
13. Bayer I, Groth P and Schneckener S: Prediction errors in learning drug response from gene expression data-influence of labeling, sample size, and machine learning algorithm. PLoS One 8: e70294, 2013.
14. Bade BC and Cruz CS: Lung Cancer 2020: Epidemiology, etiology, and prevention. Clin Chest Med 41: 1-24, 2020.
15. Nasim F, Sabath BF and Eapen GA: Lung cancer. Med Clin North Am 103: 463-473, 2019.
16. Zhou J, Xu Y, Liu J, Feng L, Yu J and Chen D: Global burden of lung cancer in 2022 and projections to 2050: Incidence and mortality estimates from GLOBOCAN. Cancer Epidemiol 93: 102693, 2024.
17. Elshaer M, Chen Y, Wang XJ and Tang X : Resveratrol: An overview of its anticancer mechanisms. Life Sci 207: 340-349, 2018.
18. Jara P, Spies J, Cárcamo C, Arancibia Y, Vargas G, Martin C, Salas M, Otth C and Zambrano A: The effect of resveratrol on cell viability in the burkitt's lymphoma cell line ramos. Molecules 23: 0014, 2017.
19. Huang XT, Li X, Xie ML, Huang Z, Huang YX, Wu GX, Peng ZR, Sun YN, Ming QL, Liu YX, *et al*: Resveratrol: Review on its discovery, anti-leukemia effects and pharmacokinetics. Chem Biol Interact 306: 29-38, 2019.
20. Li KX, Ji MJ and Sun HJ: An updated pharmacological insight of resveratrol in the treatment of diabetic nephropathy. Gene 780: 145532, 2021.
21. Vestergaard M and Ingmer H: Antibacterial and antifungal properties of resveratrol. Int J Antimicrob Agents 53: 716-723, 2019.
22. Tian B and Liu J: Resveratrol: A review of plant sources, synthesis, stability, modification and food application. J Sci Food Agric 100: 1392-1404, 2020.
23. Brockmueller A, Buhrmann C, Moravejolahkami AR and Shakibaei M: Resveratrol and p53: How are they involved in CRC plasticity and apoptosis?. J Adv Res 66: 181-195, 2024.
24. Ren B, Kwah MX, Liu C, Ma Z, Shanmugam MK, Ding L, Xiang X, Ho PC, Wang L, Ong PS and Goh BC: Resveratrol for cancer therapy: Challenges and future perspectives. Cancer Lett 515: 63-72, 2021.
25. Ahmadi R and Ebrahimzadeh MA: Resveratrol-A comprehensive review of recent advances in anticancer drug design and development. Eur J Med Chem 200: 112356, 2020.
26. Rauf A, Imran M, Butt MS, Nadeem M, Peters DG and Mubarak MS: Resveratrol as an anticancer agent: A review. Crit Rev Food Sci Nutr 58: 1428-1447, 2018.
27. Dixon SJ and Olzmann JA: The cell biology of ferroptosis. Nat Rev Mol Cell Biol 25: 424-442, 2024.
28. Wang X, Shen T, Lian J, Deng K, Qu C, Li E, Li G, Ren Y, Wang Z, Jiang Z, *et al*: Resveratrol reduces ROS-induced ferroptosis by activating SIRT3 and compensating the GSH/GPX4 pathway. Mol Med 29: 137, 2023.
29. Liu Y, Lu S, Wu LL, Yang L, Yang L and Wang J: The diversified role of mitochondria in ferroptosis in cancer. Cell Death Dis 14: 519, 2023.
30. Dixon SJ, Lemberg KM, Lamprecht MR, Skouta R, Zaitsev EM, Gleason CE, Patel DN, Bauer AJ, Cantley AM, Yang WS, *et al*: Ferroptosis: An iron-dependent form of nonapoptotic cell death. Cell 149: 1060-1072, 2012.
31. Zhou Q, Meng Y, Li D, Yao L, Le J, Liu Y, Sun Y, Zeng F, Chen X and Deng G: Ferroptosis in cancer: From molecular mechanisms to therapeutic strategies. Signal transduction and targeted therapy 9: 55, 2024.
32. Mou Y, Wang J, Wu J, He D, Zhang C, Duan C and Li B: Ferroptosis, a new form of cell death: Opportunities and challenges in cancer. J Hematol Oncol 12: 34, 2019.
33. Rochette L, Dogon G, Rigal E, Zeller M, Cottin Y and Vergely C: Lipid peroxidation and iron metabolism: Two corner stones in the homeostasis control of ferroptosis. Int J Mol Sci 24: 449, 2022.
34. Zhang H, Ma J, Hou C, Luo X, Zhu S, Peng Y, Peng C, Li P, Meng H, Xia Y, *et al*: A ROS-mediated oxidation-O-GlcNAcylation cascade governs ferroptosis. Nat Cell Biol 27: 1288-1300, 2025.
35. Wang B, Wang Y, Zhang J, Hu C, Jiang J, Li Y and Peng Z: ROS-induced lipid peroxidation modulates cell death outcome: Mechanisms behind apoptosis, autophagy, and ferroptosis. Arch Toxicol 97: 1439-1451, 2023.
36. Niu B, Liao K, Zhou Y, Wen T, Quan G, Pan X and Wu C: Application of glutathione depletion in cancer therapy: Enhanced ROS-based therapy, ferroptosis, and chemotherapy. Biomaterials 277: 121110, 2021.
37. Lee M, Cho T, Jantaratnotai N, Wang YT, McGeer E and McGeer PL: Depletion of GSH in glial cells induces neurotoxicity: Relevance to aging and degenerative neurological diseases. FASEB J 24: 2533-2545, 2010.
38. Franco R, Dehaven WI, Sifre MI, Bortner CD and Cidlowski JA: Glutathione depletion and disruption of intracellular ionic homeostasis regulate lymphoid cell apoptosis. J Biol Chem 283: 36071-36087, 2008.

Copyright © 2026 Wu et al. This work is licensed under a Creative Commons Attribution-NonCommercial-NoDerivatives 4.0 International (CC BY-NC-ND 4.0) License.